

# Improved endothelial cell adhesion and proliferation on patterned titanium surfaces with rationally designed, micrometer to nanometer features

Jing Lu <sup>a</sup>, Masaru P. Rao <sup>b,c,d,e</sup>, Noel C. MacDonald <sup>f</sup>,  
Dongwoo Khang <sup>a</sup>, Thomas J. Webster <sup>a,\*</sup>

<sup>a</sup> Division of Engineering and Department of Orthopaedic Surgery, Brown University, Providence, RI 02912, USA

<sup>b</sup> School of Mechanical Engineering, Purdue University, West Lafayette, IN 47907, USA

<sup>c</sup> School of Materials Engineering, Purdue University, West Lafayette, IN 47907, USA

<sup>d</sup> Birck Nanotechnology Center, Purdue University, West Lafayette, IN 47907, USA

<sup>e</sup> Center for Advanced Manufacturing, Purdue University, West Lafayette, IN 47907, USA

<sup>f</sup> Department of Mechanical Engineering, University of California, Santa Barbara, CA 93106, USA

Received 29 April 2007; received in revised form 4 June 2007; accepted 8 July 2007

Available online 2 August 2007

## Abstract

Previous *in vitro* studies have demonstrated increased vascular endothelial cell adhesion on random nanostructured titanium (Ti) surfaces compared with conventional (or nanometer smooth) Ti surfaces. These results indicated for the first time the potential nanophase metals have for improving vascular stent efficacy. However, considering the structural properties of the endothelium, which is composed of elongated vascular endothelial cells aligned with the direction of blood flow, it has been speculated that rationally designed, patterned nano-Ti surface features could further enhance endothelial cell functions by promoting a more native cellular morphology. To this end, patterned Ti surfaces consisting of periodic arrays of grooves with spacings ranging from 750 nm to 100  $\mu$ m have been successfully fabricated in the present study by utilizing a novel plasma-based dry etching technique that enables machining of Ti with unprecedented resolution. *In vitro* rat aortic endothelial cell adhesion and growth assays performed on these substrates demonstrated enhanced endothelial cell coverage on nanometer-scale Ti patterns compared with larger micrometer-scale Ti patterns, as well as controls consisting of random nanostructured surface features. Furthermore, nanometer-patterned Ti surfaces induced endothelial cell alignment similar to the natural endothelium. Since the re-establishment of the endothelium on vascular stent surfaces is critical for stent success, the present study suggests that nanometer to submicrometer patterned Ti surface features should be further investigated for improving vascular stent efficacy.

© 2007 Acta Materialia Inc. Published by Elsevier Ltd. All rights reserved.

**Keywords:** Patterning; Titanium; Endothelial cells; Stents; Morphology

## 1. Introduction

Coronary heart disease (CHD) is the leading cause of death worldwide, killing over 7 million people per year, which represents 1 in every 7 deaths [1]. It is characterized by arterial narrowing (stenosis) due to the accumulation of

fatty deposits beneath the endothelium (i.e. the layer of cells which forms the inner lining of a blood vessel [2]). This accumulation, known as atherosclerosis, can cause restriction of blood flow, thus depriving heart muscles and other tissues of oxygen. In severe cases of atherosclerosis, stent implantation has become the preferred method for restoring normal blood flow [3].

Stents are commonly metallic, lattice-like scaffolds that are inserted into stenosed arteries to maintain or re-estab-

\* Corresponding author. Tel.: +1 401 863 2318; fax: +1 401 863 1001.  
E-mail address: [Thomas\\_Webster@Brown.edu](mailto:Thomas_Webster@Brown.edu) (T.J. Webster).

lish vascular patency. In their first embodiment, they simply served as mechanical support systems to prevent vascular elastic recoil. However, they have since evolved to incorporate biological functionality (such as impregnation of pharmaceutical drugs) in order to mitigate neointimal hyperplasia and decrease immune responses initiated by the injury created through stent implantation. This detrimental immune response is characterized by excessive tissue in-growth into the lumen, which can cause re-narrowing of arteries over time (restenosis) [4–6]. As detailed in recent reviews [7–14], considerable effort has been dedicated to addressing this issue. However, the most successful solution to date has been the drug-eluting stent (DES), which relies on the delivery of anti cell-proliferative drugs from a polymer coating on the stent; such drugs inhibit cellular responses which lead to hyperplasia. In clinical trials, DES has been shown to significantly reduce restenosis relative to bare-metal stents [15,16]. Consequently, DES adoption has been rapid and widespread since FDA approval in 2002.

However, despite the success of DES, recent studies have begun to question the wisdom of a therapeutic strategy effectively based on the inhibition of healing. In particular, there is growing evidence that the incidence of stent-related thrombosis (i.e. clotting) is higher in DES than bare-metal stents, particularly after cessation of adjunctive anti-platelet therapy. Moreover, the incidence of stent-related thrombosis increases considerably when there is premature discontinuation of such therapies [17–27]. While overall incidences of stent-related thrombosis in DES is low (<1.5%), these results provide significant cause for concern because the fatalities in such cases can be as high as 45% [22]. Although the mechanism of stent-related thrombosis has yet to be fully understood, a causal relationship between DES and delayed healing has been established. Most significantly, drug-induced inhibition of hyperplasia also inhibits the re-establishment of a healthy endothelium; thus, such approaches increase the potential for thrombogenic stimuli [28,19,23]. This, therefore, provides the impetus for the exploration of alternative therapeutic strategies that enhance, rather than inhibit, endothelialization of metallic stent surfaces.

In this light, a number of studies have begun to show the promise of healing-based strategies for increasing vascular stent efficacy. All presume that rapid restoration of the endothelium over the stent will enable its isolation from circulating blood, and therefore reduce the potential for restenosis and thrombosis. To date, most have focused on the use of bioactive agents (such as growth factors, peptides, and antibodies) which have been delivered locally via coating-based elutions, surface-immobilizations, or porous balloon catheters [28–35]. However, as in DES, the efficacy of such approaches is often critically dependent upon spatial and/or temporal control of bioactive agent delivery. Moreover, consideration must also be given to the potentially detrimental consequences of unintended systemic delivery [36,37]. Thus, the focus of this study was to develop tech-

niques that can increase endothelialization without the use of bioactive agents.

One approach that seems promising in this context is the creation of nanoscale features on vascular metallic stent surfaces which mimic the natural structure of the healthy vessel wall. Choudhary et al. recently showed greater vascular cell adhesion on metal surfaces with random nanostructured features [38]. It was demonstrated that metals with random nanostructured surface features invoked vascular cell responses promising for improving stent efficacy [38]. However, since native endothelial cells adopt an elongated, aligned morphology in the vasculature, it can be argued that patterned surface features on metallic stents may be better for increasing endothelial cell functions. Thus, the objective of this *in vitro* study was to investigate endothelial cell function on surfaces with rationally designed patterns composed of periodic arrays of nanometer-wide grooves compared with both micrometer-wide grooves and no grooves at all.

## 2. Materials and methods

### 2.1. Fabrication of patterned titanium substrates

Plasma dry etching-based micromachining techniques were used to define uniform, high-precision patterns on the surface of titanium substrates in the present study. Wafer-based substrates composed of polished grade 1 Ti (99.6% Ti, Tokyo Stainless Grinding Co., Ltd., Japan,  $R_A \sim 10$  nm RMS) were first cleaned in subsequent ultrasonic baths of acetone and isopropanol, followed by rinsing with deionized (DI) water and drying with  $N_2$  gas. The wafers were then dehydration baked on a hotplate at 150 °C for 3 min. The wafers were primed with hexamethyldisilazane (an adhesion promoter) and a layer photoresist (Shipley SPR 955) was applied by spin-coating. After lithographic exposure (GCA 6300 i-line wafer stepper), the wafers were baked at 95 °C for 60 s, then developed (Shipley MF 701) for 60 s, rinsed in DI water and dried with  $N_2$  gas.

The lithographically defined patterns in the present study were composed of nine  $5 \times 5$  mm<sup>2</sup> subregions, each of which was composed of a periodic array of lines of equal width and spacing ranging from 750 nm to 100  $\mu$ m. A different line width was used for each subpattern, thus enabling the definition of nine unique topographical regions within the same die. The photoresist patterns were transferred into the underlying substrate using the titanium inductively coupled plasma deep etch (TIDE) process [39]. The TIDE process is based on anisotropic dry etching of Ti in  $Cl_2/Ar$  plasma. It provides, for the first time, the capability for machining Ti with unprecedented resolution in a manner that is intrinsically scalable to low-cost/high-volume manufacturing, owing to its reliance on batch processing techniques derived from the microelectronics industry. Following etching, the photoresist was stripped using ultrasonic agitation, first in acetone, then in isopropanol. The samples were then rinsed in DI and dried with  $N_2$  gas.

## 2.2. Fabrication of control materials

Three types of controls were used in the current study: (i) smooth titanium; (ii) titanium with random nanostructured surface features; and (iii) glass coverslips. The smooth Ti samples were unpatterned versions of the polished substrates used for the patterned samples. The random nanostructured control samples were thin discs (12 mm diameter, 0.5 mm thickness) created by cold compaction of 99.38% commercially pure Ti nanopowders (average particle size: 100 nm, Reade International Inc.) according to standard techniques [40]. Briefly, nanopowders were loaded into a hardened tool steel die and compacted using a uniaxial, single-ended hydraulic press (Carver Inc.; compaction conditions: 10 GPa pressure, 10 min at room temperature in an ambient environment). The glass coverslip (Fisher) control samples were prepared by etching in a 1 N NaOH solution for 1 h.

Before cell culture experiments, all substrates were rinsed in acetone for 5 min, ethanol for 5 min and finally DI water for another 5 min. They were then sterilized by autoclaving (115–120 °C) for 30 min.

## 2.3. Substrate characterization

Scanning electron microscopy (SEM; LEO 1530 VP) was used to characterize the surfaces of the patterned Ti substrates. Prior to imaging, the substrates were sputter-coated with a thin layer of gold–palladium in a 100 mTorr vacuum argon environment for 3 min using a current of 100 mA. SEM imaging was performed at 5 kV accelerating voltage. It should be noted that these sputter-coated samples were not used for subsequent cell culture experiments.

The surface topography of the patterned Ti substrates was further characterized by atomic force microscopy (AFM; Dimension™ 3100, Nanoscope IIIa). Commercially available AFM tips (radius of tip curvature <10 nm, NSC15/ALBS, MikroMasch) were used in tapping mode. Tips with a full tip cone angle of <10° in the last 200 nm of the tip apex were used (25 µm full tip height, 30° full cone angle after initial 200 nm, 40 N m<sup>-1</sup> force constant). The scan rate was fixed at 0.5 Hz.

## 2.4. Endothelial cell culture

To test the endothelial cell responses on the patterned Ti, rat aortic endothelial cells (RAEC) were purchased from VEC Technologies. For culturing, Petri dishes were coated with 0.2% gelatin (Sigma) by immersion in 0.2% gelatin for 2 h at room temperature, followed by air drying in a laminar flow hood for 12 h. RAEC were then cultured in MCDB-131 Complete Medium (VEC Technologies) under standard cell culture conditions (37 °C, humidified, 5% CO<sub>2</sub>/95% air environment). Fresh medium was replenished every other day.

## 2.5. Endothelial cell adhesion and cell density assays

For initial cell adhesion tests, RAEC were seeded at 4500 cells cm<sup>-2</sup> in MCDB-131 Complete Medium onto the substrates for 4 h under standard cell culture conditions. The samples were then rinsed with phosphate-buffered saline (PBS) three times to remove non-adherent cells to prepare them for cell viability analysis.

For longer-term cell density assays, RAEC were seeded at 2500 cells cm<sup>-2</sup> in MCDB-131 Complete Medium onto the substrates. Cells were cultured for 1, 3 and 5 days. Medium was refreshed on days 2 and 4. At the end of days 1, 3 and 5, non-adherent cells on all the substrates were removed by rinsing three times with PBS to prepare them for cell viability analysis.

Cell viability was determined in situ by a LIVE/DEAD Viability/Cytotoxicity Kit for mammalian cells (Molecular Probes). Briefly, the cells were stained with 3.3 µM of calcein AM and 1.7 µM of ethidium homodimer-1 and incubated for 30 min before visualization using fluorescence microscopy. The live and dead cells were counted using 530 nm wavelength excitation for calcein AM and 560 nm for ethidium homodimer-1. Five random fields were counted per substrate area of interest. Experiments were conducted in triplicate and repeated at three different times.

Endothelial cell morphology on the substrates after the 5 day assay was also quantified using SEM. Briefly, after the prescribed time period, endothelial cells were fixed with formalin for 5 min. Afterwards, they were dehydrated by soaking serially in 10%, 30%, 50%, 70% and 90% ethanol for 30 min followed by soaking in 100% ethanol for 15 min three times. Lastly, the substrates were critical point dried before visualization.

## 3. Results

### 3.1. Patterned substrate topographical characterization

Scanning electron micrographs (Fig. 1) and AFM images (Fig. 2) demonstrated the high-resolution patterning capability of the TIDE process. Periodic arrays of uniform grooves with nearly vertical sidewalls were created with widths and spacings ranging from hundreds of nanometers (750 nm) to many tens of micrometers. The sporadic thin bright lines and spots observed in the etched grooves (darker stripes) of the SEM micrographs (Fig. 1) of the patterned samples are artifacts due to the dry etching process. They were caused by the presence of impurities in the titanium substrate material that were not etched by the Cl<sub>2</sub>/Ar plasma. Their incidence decreased considerably with decreasing feature size and they were virtually non-existent in the nanometer patterned samples.

### 3.2. Endothelial cell adhesion after 4 h on patterned Ti

Results from the 4 h endothelial cell adhesion tests indicated that endothelial cell density increased significantly as

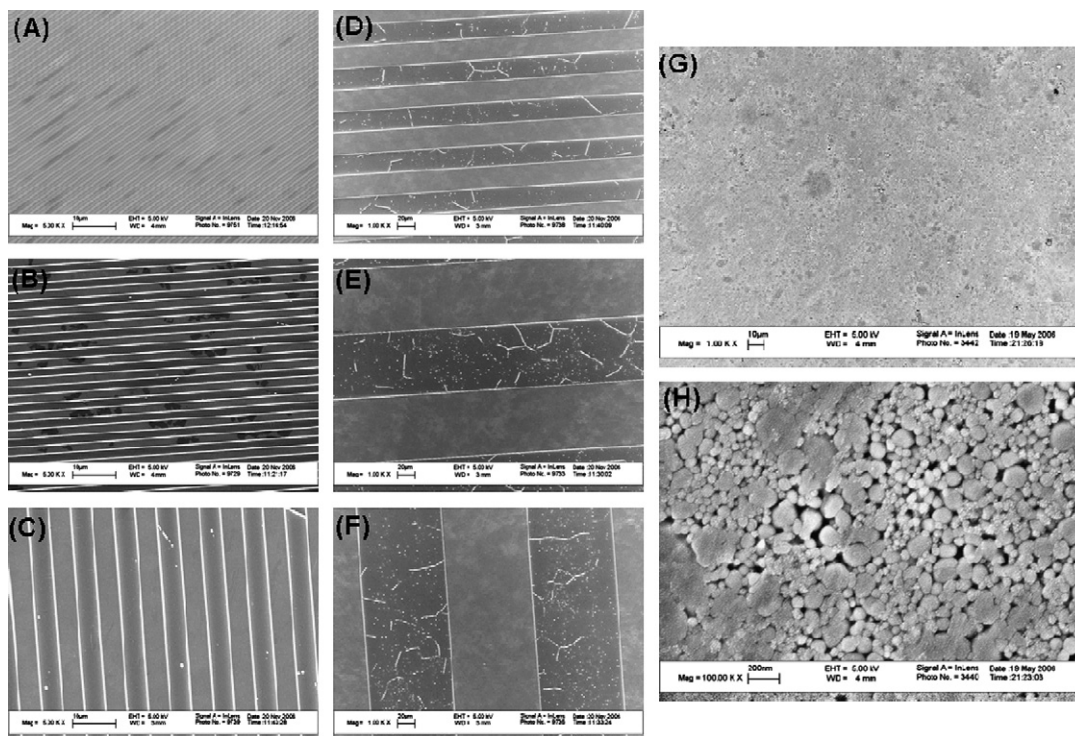


Fig. 1. Scanning electron microscope (SEM) images of Ti patterned surface features of: (A) 750 nm, bar = 1  $\mu\text{m}$ ; (B) 2  $\mu\text{m}$ , bar = 1  $\mu\text{m}$ ; (C) 5  $\mu\text{m}$ , bar = 1  $\mu\text{m}$ ; (D) 25  $\mu\text{m}$ , bar = 20  $\mu\text{m}$ ; (E) 75  $\mu\text{m}$ , bar = 20  $\mu\text{m}$ ; and (F) 100  $\mu\text{m}$ , bar = 20  $\mu\text{m}$ ; random nanostructured surface features of (G) bar = 10  $\mu\text{m}$  and (H) bar = 200 nm. The thin, non-uniform bright lines and spots observed in the etched grooves (darker stripes) are artifacts of the dry etching process.

the Ti pattern dimensions decreased to the nanometer scale (Fig. 3). Moreover, when compared with the cell density on the random nanostructured and smooth Ti surfaces, endothelial cell density was greater on the nanopatterned Ti surfaces. The cells also began to spread and align on the nanopatterned Ti surfaces when the dimensions were less than 10  $\mu\text{m}$  (Fig. 4); this was not observed on larger micropatterned Ti samples, nor on the random nanostructured Ti, smooth Ti or glass control surfaces.

### 3.3. Endothelial cell density after 1, 3 and 5 days on patterned Ti

Longer-term cultures demonstrated similar trends as observed for the 4 h cultures. Specifically, endothelial cell density on the 750 nm patterned Ti surfaces was twice that on the 100  $\mu\text{m}$  patterned surfaces after 1 day (Fig. 5) and cellular alignment increased considerably with decreasing feature size (Fig. 6). After 3 days, endothelial cell density continued to be greater on the Ti patterns with feature size less than 10  $\mu\text{m}$  (Fig. 7). Furthermore, cellular alignment and elongation was far more pronounced for patterns with features less than 10  $\mu\text{m}$ .

Importantly, endothelial cells formed a confluent layer on all patterned Ti substrates before completion of the 5 day culture experiments (Fig. 8). In contrast, confluence was not achieved after 5 days for any of the control surfaces (i.e. smooth Ti, random nanostructured Ti, or glass). Furthermore, confluence occurred most quickly on the Ti

surfaces with patterns less than 10  $\mu\text{m}$ , with the 750 nm patterns reaching confluence first. Finally, the affect of decreasing pattern feature size on cellular alignment and morphology is demonstrated in Fig. 9. The length/width ratio of the endothelial cells on the 1  $\mu\text{m}$  patterns is considerably greater than those on the 100  $\mu\text{m}$  patterns.

## 4. Discussion

This in vitro study represents the first exploration of endothelial cell adhesion, proliferation and morphology on rationally designed patterned Ti surfaces composed of periodic arrays of grooves with width and spacing ranging from 750 nm to 100  $\mu\text{m}$ . The data demonstrated superior endothelial cell function and orientation on patterned Ti surfaces relative to all other surfaces investigated (i.e. smooth Ti, random nanostructured Ti and glass). Moreover, the data demonstrated increasing benefits with decreasing pattern feature sizes, thus suggesting that even greater promise may lie in further feature size reduction. It should be noted, however, that these results are not necessarily indicative of the potential for success in vivo, due to the complexity of the in vivo environment. As such, further studies are ongoing to assess the effects of competitive adhesion with vascular smooth muscle cells in vitro as well as the translation of these results to an in vivo environment. Successful outcomes of these experiments will provide further evidence of the promise of this approach.

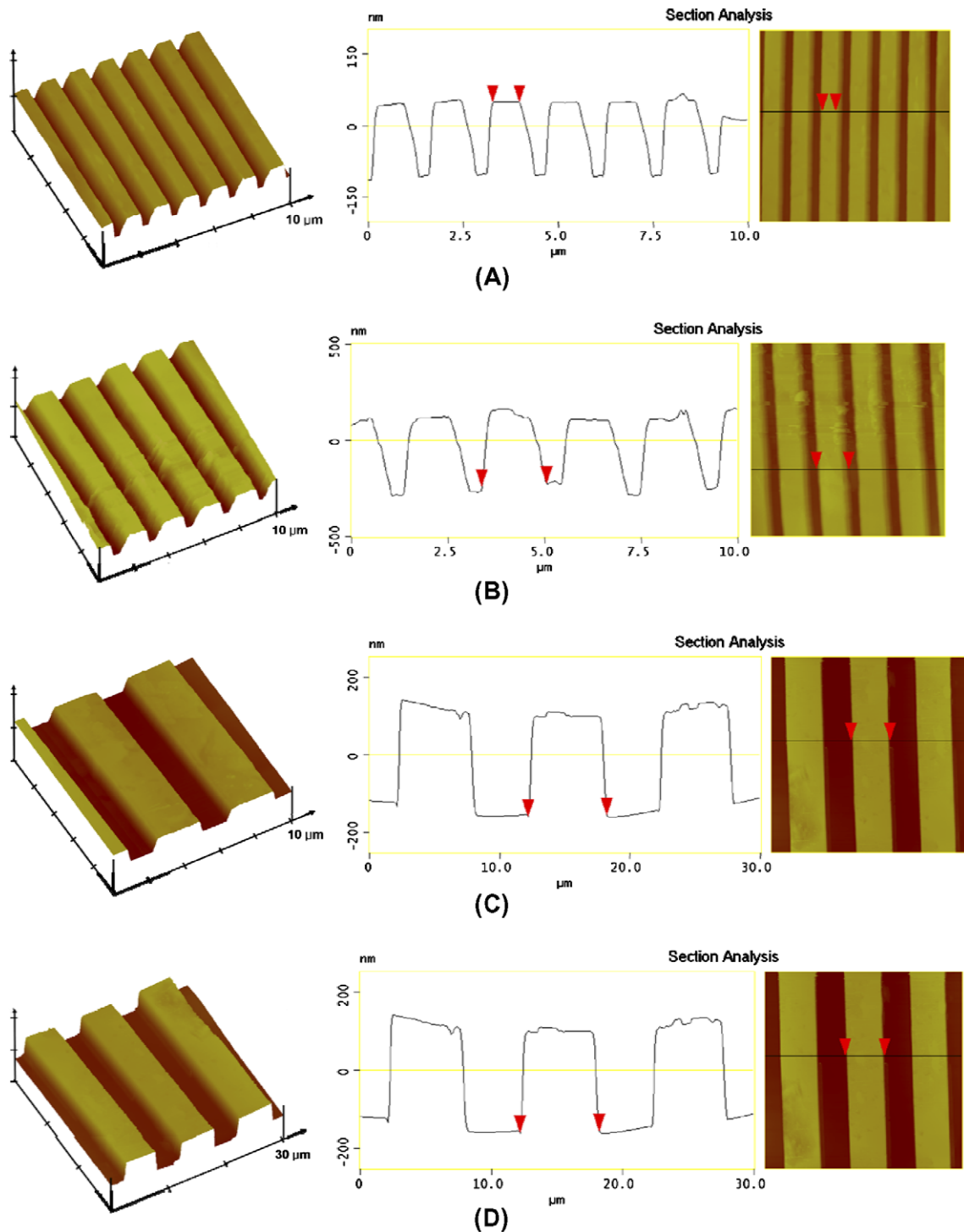


Fig. 2. Atomic force microscope (AFM) images of Ti patterned surface features of: (A) 750 nm, scan scale = 10  $\mu\text{m}$ ; (B) 1  $\mu\text{m}$ , scan scale = 10  $\mu\text{m}$ ; (C) 2  $\mu\text{m}$ , scan scale = 10  $\mu\text{m}$  and (D) 5  $\mu\text{m}$ , scan scale = 30  $\mu\text{m}$ .

Importantly, this study introduces a new technique that can produce, with high precision and reproducibility, nanometer to micrometer-scale surface features on Ti. When coupled with high-resolution lithographic patterning, the gentle, molecular-scale material removal mechanism of the TIDE process enables machining at a far smaller scale than is possible with conventional stent machining tech-

niques (such as laser micromachining (LMM), photoetching and microelectrodischarge machining ( $\mu\text{EDM}$ ), all of which are limited to minimum feature sizes in excess of tens of micrometers in practice [41,42]). However, plasma etching also compares favorably to these techniques on the micro/mesoscale. TIDE is a parallel, batch-scale process, thus making it inherently scalable to

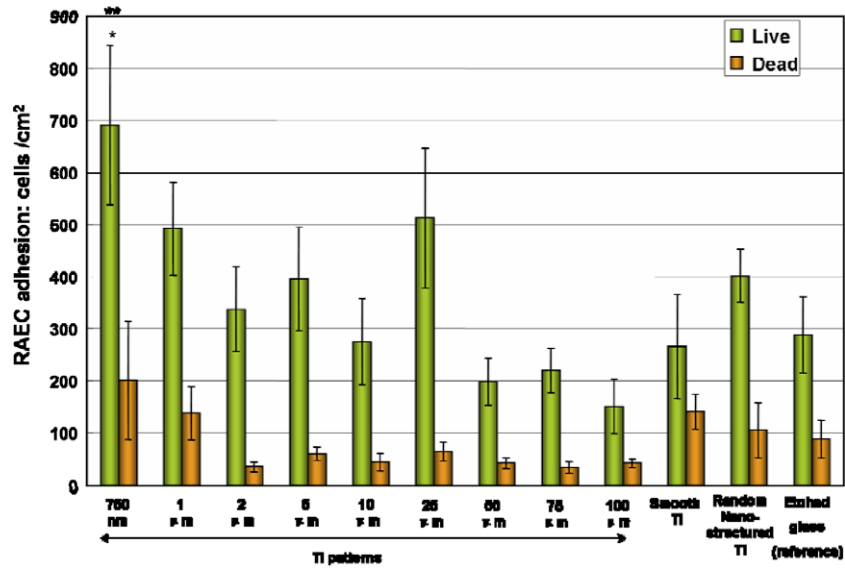


Fig. 3. Increased rat aortic endothelial cell (RAEC) adhesion after four hour culture on nano to sub-micrometer patterns compared to micrometer-scale patterns and random nanostructured Ti features. Data = mean ± SEM; *N* = 6; \*,\*\**p* < 0.01 (compared to Ti patterns of 100 μm and random nanostructured Ti, respectively).

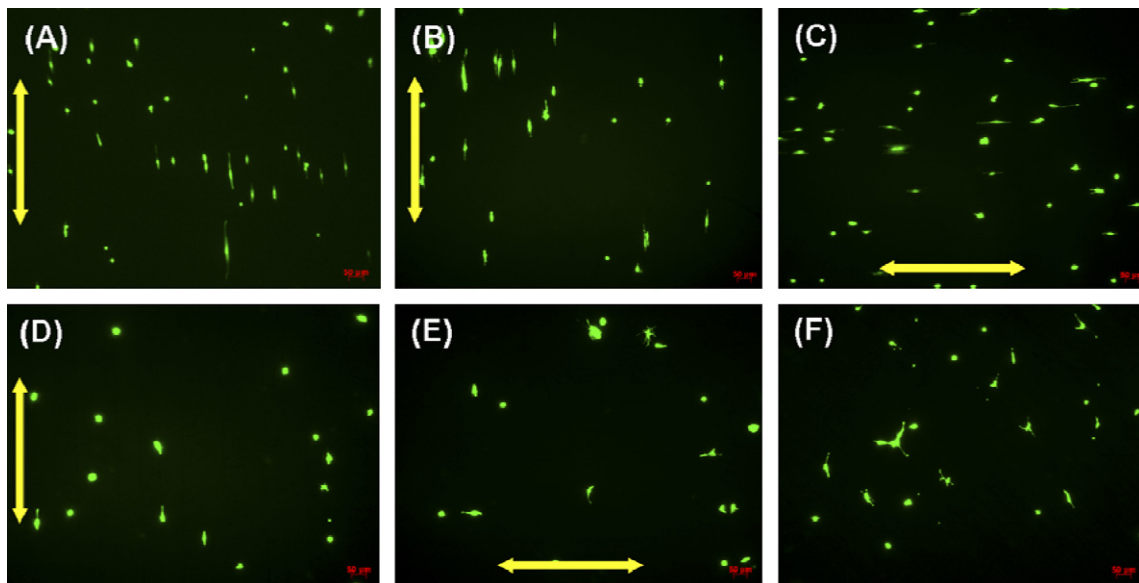


Fig. 4. Rat aortic endothelial cell (RAEC) cell density after four hours of culture on Ti patterns of (A) 750 nm; (B) 2 μm; (C) 5 μm; (D) 75 μm; (E) 100 μm and (F) random nanostructured Ti surfaces. (A–F) bars = 50 μm. Arrows indicate groove alignment direction on patterned samples.

low-cost/high-volume manufacturing, unlike LMM and μEDM, which are slower, serial processes. Furthermore, in addition to providing higher-resolution machining capability, lithographic patterning also enables better tolerances and reproducibility than what is possible with conventional techniques, thus ensuring greater quality control and reliability. Finally, the gentle machining mechanism of plasma etching produces little or no debris or damage, thus minimizing the need for common post-machining processes, such as electropolishing. As such, the TIDE process is the only technique currently available that has the potential to produce nanometer to micrometer-scale patterning in stents in a reliable and cost-effective manner.

Clearly, it is important to consider the mechanism of why endothelial cell responses were improved on these nanopatterned Ti surfaces. Although not directly addressed here, other studies have attributed improved cellular responses on nano- to submicron-scale patterned surfaces to a physical effect; that is, changes in the alignment and shape of cells (as controlled by the underlying surface features) have been related to improved cell functions [43]. For example, Palmaz et al. have reported higher endothelial cell migration rates on Nitinol surfaces consisting of micrometer-scale grooves compared with smooth metal surfaces [44]. They hypothesized that such patterns may reduce time to endothelialization of vascular stents, thus

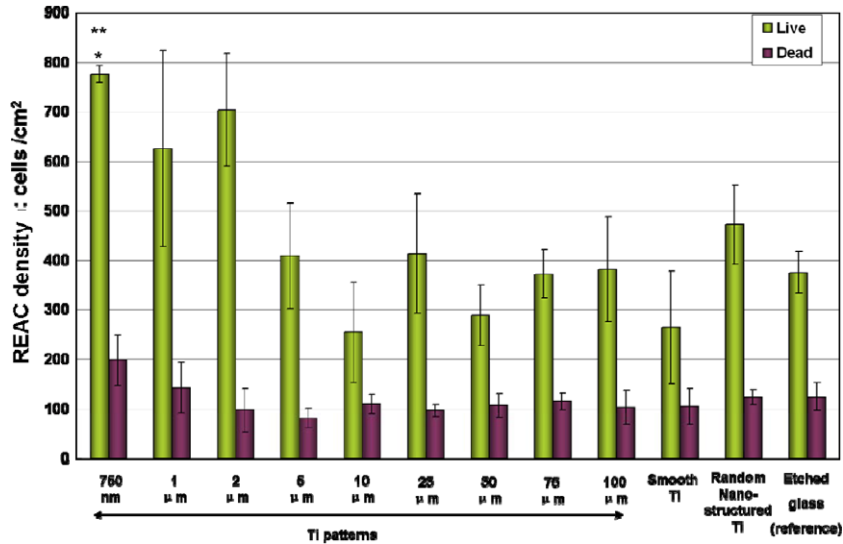


Fig. 5. Increased rat aortic endothelial cell (RAEC) cell density after the first day of culture on patterned Ti surface features. Data = mean  $\pm$  SEM;  $N = 3$ ; \* $p < 0.05$  (compared to the patterns of 100 and 75  $\mu\text{m}$ ) and \*\* $p < 0.05$  (compared to random nanostructured surface features).

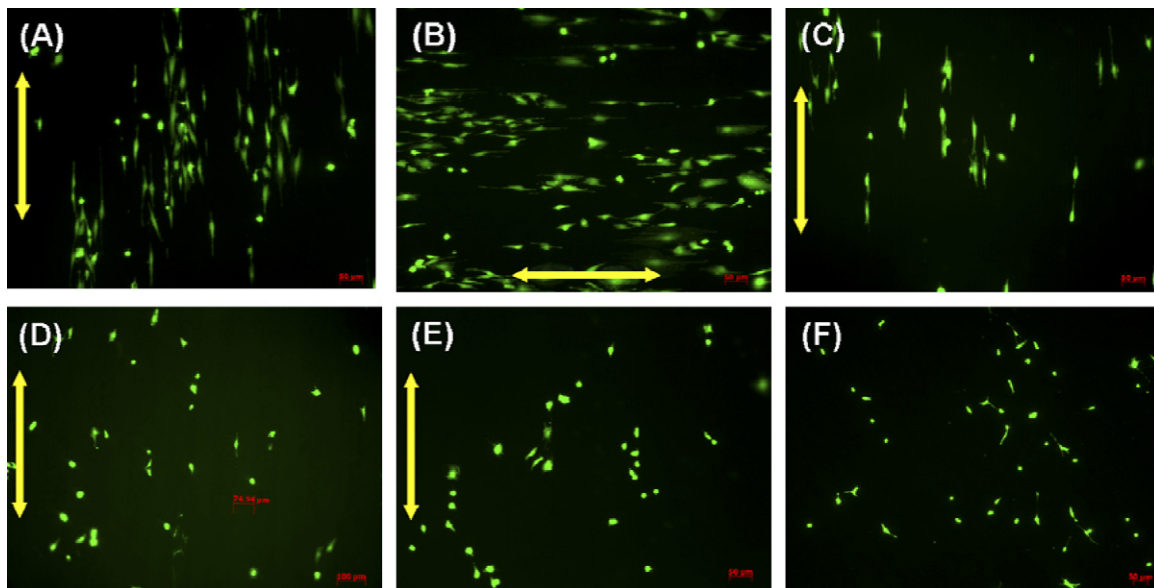


Fig. 6. Rat aortic endothelial cell (RAEC) cell density after the first day of culture on Ti patterns of: (A) 750 nm; (B) 2  $\mu\text{m}$ ; (C) 5  $\mu\text{m}$ ; (D) 75  $\mu\text{m}$ ; (E) 100  $\mu\text{m}$  and (F) random nanostructured Ti surfaces. (A–F) bars = 50  $\mu\text{m}$ . Arrows indicate groove alignment direction on patterned samples.

reducing the risk of in-stent restenosis and late-stage thrombosis [44]. They attributed this increase to a physical effect; that is, changes in the alignment and shape of cells were related to a simple cell conformation process on the microgrooves. Other studies have confirmed that cell shape and orientation are related to cell gene expression [45]. Changes in cell shape may thus affect much of the metabolism of a cell.

However, there is some contradiction in the literature concerning the influence of surface patterns on cell alignment. While there has been only limited exploration of this for nano- to submicrometer-scale surface features [46], this has been extensively studied for materials with micrometer-

scale or greater surface features. Some studies have indicated that the degree of cell alignment increases with groove size [48], while others show that the higher the concentration of ridges on the grooved surface, the greater the effect on cell morphology [47]. Consequently, it is apparent that the influence of the dimensions of surface patterning is another important subject to be studied further in which unique enhancements may be made when going down to the nanoscale, as this study suggests.

The data presented here clearly indicate a strong enhancement of endothelial cell function with decreasing pattern feature sizes into the nanometer regime. As such, within the context of the application towards improving

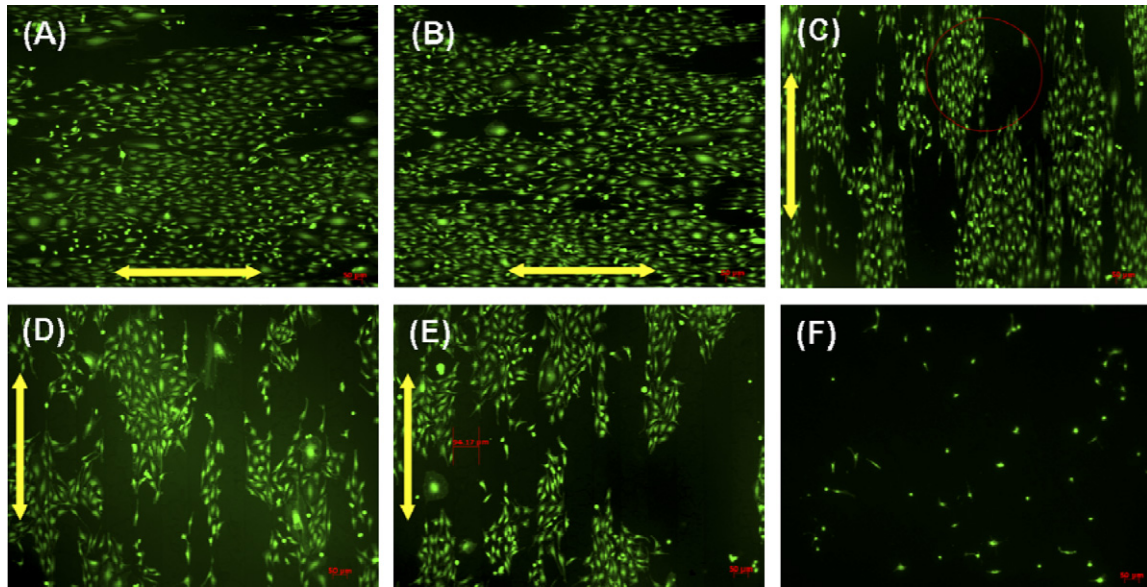


Fig. 7. Rat aortic endothelial cell (RAEC) cell density after the third day of culture on Ti patterns of (A) 750 nm; (B) 1  $\mu\text{m}$ ; (C) 5  $\mu\text{m}$ ; (D) 75  $\mu\text{m}$ ; (E) 100  $\mu\text{m}$  and (F) random nanostructured Ti surfaces. (A–F) bars = 50  $\mu\text{m}$ . Arrows indicate groove alignment direction on patterned samples.

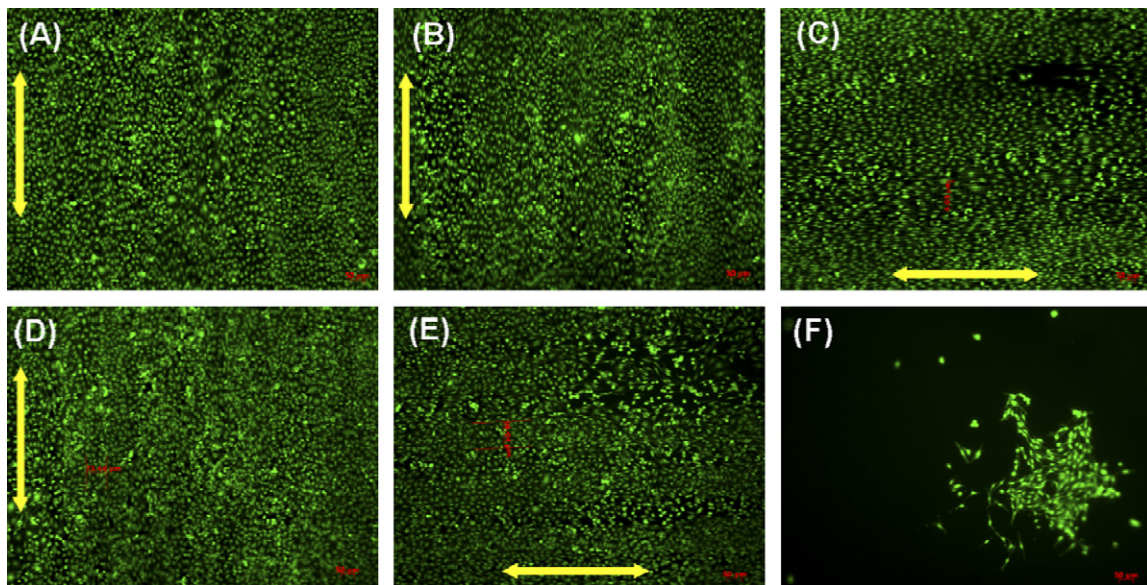


Fig. 8. Rat aortic endothelial cell (RAEC) proliferation after the fifth day of culture on Ti patterns of: (A) 750 nm; (B) 2  $\mu\text{m}$ ; (C) 5  $\mu\text{m}$ ; (D) 75  $\mu\text{m}$ ; (E) 100  $\mu\text{m}$  and (F) random nanostructured Ti surfaces. (A–F): bars = 50  $\mu\text{m}$ . Arrows indicate groove alignment direction on patterned samples.

vascular stents, this approach may offer a unique opportunity. The inherent precision and uniformity of the fabrication method used to create the patterned surfaces may enable better control and reproducibility of cellular responses than uncontrolled surfaces whose spatial uniformity may vary widely. Moreover, patterning of the surface of the stent material itself may enable incorporation of multi-functionality based solely on the rational design of stent structures at varying length scales. More specifically, micro- and mesoscale stent features would define the mechanical response of the stent, while nano- to submicrometer-scale topographical features would define its

biological response. No other materials or agents would be needed (such as the aforementioned pharmaceutical agents which inhibit a healing response). If successful, a monolithic integration approach (such as this) has the potential to be inherently more reliable than current multi-component approaches employing pharmaceutical agents.

Finally, although beyond the scope of the current study, it is anticipated that patterning at the nanometer and micrometer scale via the TIDE process will find similar utility in other implantation applications as well. For example, cues provided by nanopatterned surface features could

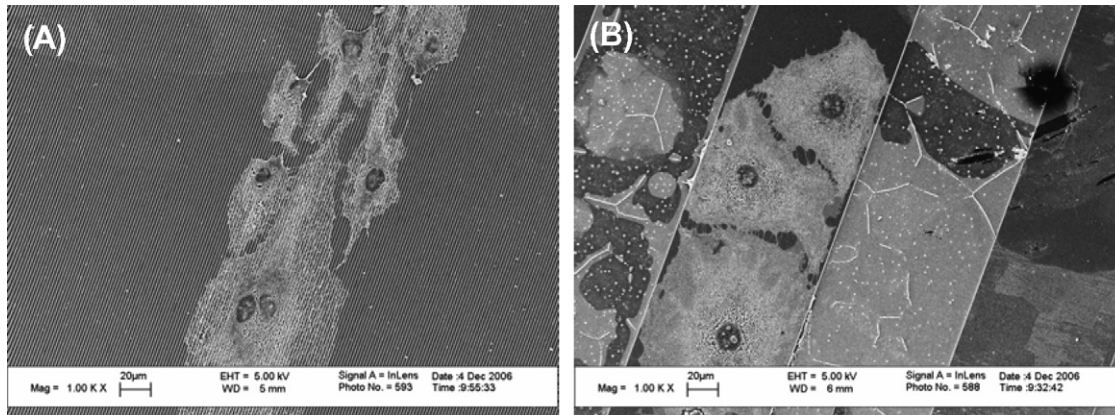


Fig. 9. SEM images of rat aortic endothelial cell (RAEC) morphology after the fifth day of culture on Ti patterns of: (A) 1  $\mu\text{m}$ ; (B) 100  $\mu\text{m}$ . Bars = 20  $\mu\text{m}$ .

facilitate the orientation of deposited calcium containing minerals and collagen by bone-forming cells, thus improving integration of orthopaedic implants. Indeed, evidence of this has already been demonstrated at the micrometer scale, where the formation of bone-like cell multilayers was observed to occur more quickly on microgrooved surfaces (150  $\mu\text{m}$ ) than smooth surfaces [48]. However, the effect of nanopatterned surfaces (as the TIDE process could provide) has yet to be investigated.

## 5. Conclusions

In summary, rationally designed patterned Ti surfaces with features ranging from 750 nm to 100  $\mu\text{m}$  have been created using a novel micromachining process which provided the capability for creating surface features with unparalleled control and resolution. These nanofeatures have been shown to promote endothelial cell function on Ti to mimic that of the native endothelium. Such results therefore suggest that nanopatterned Ti substrates should be further studied as a means of improving vascular stent efficacy.

## Acknowledgements

The authors gratefully thank the Coulter Foundation for funding, and Dr. Robbert Créton and Mr. Geoffrey Williams for help with fluorescence microscopy.

## References

- [1] Mackay J, Mensah G, editors. The atlas of heart disease and stroke. Geneva: World Health Organization; 2004.
- [2] Libby P, Ridker PM, Maseri A. Inflammation and atherosclerosis. *Circulation* 2002;105(9):1135–43.
- [3] Thom T, Haase N, Rosamond W, Howard VJ, Rumsfeld J, Manolio T, et al. Heart disease and stroke statistics – 2006 update: a report from the American Heart Association statistics committee and stroke subcommittee. *Circulation* 2006;113(6):E 85–151.
- [4] Hoffmann R, Mintz GS, Dussailant GR, Popma JJ, Pichard AD, Satler LF, et al. Patterns and mechanisms of in-stent restenosis – a serial intravascular ultrasound study. *Circulation* 1996;94(6):1247–54.
- [5] Farb A, Sangiorgi G, Carter AJ, Walley VM, Edwards WD, Schwartz RS, et al. Pathology of acute and chronic coronary stenting in humans. *Circulation* 1999;99(1):44–52.
- [6] Schwartz RS, Chronos NA, Virmani R. Preclinical restenosis models and drug-eluting stents: still important, still much to learn. *J Am Coll Cardiol* 2004;44(7):1373–85.
- [7] Palmaz JC. New advances in endovascular technology. *Texas Heart Inst J* 1997;24(3):156–9.
- [8] Topol EJ. Coronary-artery stents: gauging, gorging, and gouging [editorial]. *N Engl J Med* 1998;339(23):1702–4.
- [9] Schömig A, Kastrati A. Long lesions, long stents and the long process of stent optimization [editorial]. *J Am Coll Cardio* 1999;34(3):660–2.
- [10] Kastrati A, Hall D, Schömig A. Long-term outcome after coronary stenting [review]. *Curr Control Trials Cardiovasc Med* 2000;1(1): 48–54.
- [11] Palmaz JC, Bailey S, Marton D, Sprague E. Influence of stent design and material composition on procedural outcome. *J Vasc Surg* 2002;36(5):1031–9.
- [12] Palmaz JC. Intravascular stents in the last and the next 10 years. *J Endovasc Ther* 2004;11(suppl. 2):200–6.
- [13] Hara H, Nakamura M, Palmaz JC, Schwartz RS. Role of stent design and coatings on restenosis and thrombosis. *Adv Drug Deliver Rev* 2006;58(3):377–86.
- [14] Whittaker DR, Fillinger MF. The engineering of endovascular stent technology: a review. *Vasc Endovasc Surg* 2006;40(2):85–94.
- [15] Moses JW, Leon MB, Popma JJ, Fitzgerald PJ, Holmes DR, O’Shaughnessy C, et al. Sirolimus-eluting stents versus standard stents in patients with stenosis in a native coronary artery. *N Engl J Med* 2003;349(14):1315–23.
- [16] Stone GW, Ellis SG, Cox DA, Hermiller J, O’Shaughnessy C, Mann JT, et al. A polymer-based, paclitaxel-eluting stent in patients with coronary-artery disease. *N Engl J Med* 2004;350(3):221–31.
- [17] McFadden EP, Stabile E, Regar E, Cheneau E, Ong ATL, Kinnaird T, et al. Late thrombosis in drug-eluting coronary stents after discontinuation of antiplatelet therapy. *Lancet* 2004;364(9444): 1519–21.
- [18] Virmani R, Guagliumi G, Farb A, Musumeci G, Greico N, Motta T, et al. Localized hypersensitivity and late coronary thrombosis secondary to a sirolimus-eluting stent: should we be cautious? *Circulation* 2004;109(6):701–5.
- [19] Joner M, Finn AV, Farb A, Mont EK, Kolodgie FD, Ladisch E, et al. Pathology of drug-eluting stents in humans: delayed healing and late thrombotic risk. *J Am Coll Cardiol* 2005;48(1):193–202.
- [20] Ong ATL, McFadden EP, Regar E, de Jaegere PPT, van Domburg RT, Serruys PW. Late angiographic stent thrombosis (LAST) events with drug-eluting stents. *J Am Coll Cardiol* 2005;45(12):2088–92.
- [21] Ong ATL, Serruys PW. Drug-eluting stents: current issues [key note address]. *Texas Heart Inst J* 2005;32(3):372–7.

- [22] Iakovou I, Schmidt T, Bonizzoni E, Ge L, Sangiorgio GM, Stankovic G, et al. Incidence, predictors, and outcome of thrombosis after successful implantation of drug-eluting stents. *JAMA* 2005;293(17):2126–30.
- [23] Nebeker JR, Virmani R, Bennett CL, Hoffman JM, Samore MH, Alvarez J, et al. Hypersensitivity cases associated with drug-eluting coronary stents: a review of available cases from the research on adverse drug events and reports (RADAR) project. *J Am Coll Cardiol* 2006;47(1):175–81.
- [24] Kuchulakanti PK, Chu WW, Torguson R, Ohlmann P, Rha SW, Clavijo LC, et al. Correlates and long-term outcomes of angiographically proven stent thrombosis with sirolimus- and paclitaxel-eluting stents. *Circulation* 2006;113(8):1108–13.
- [25] Spertus JA, Kettelkamp R, Vance C, Decker C, Jones PG, Rumsfeld JS, et al. Prevalence, predictors, and outcomes of premature discontinuation of thienopyridine, therapy after drug-eluting stent placement: results from the PREMIER registry. *Circulation* 2006;113(24):2803–9.
- [26] Do drug-eluting stents increase deaths? Retrieved September 11, 2006 from European Society of Cardiology, ESC Event News, 2006 World Congress of Cardiology. <[http://www.escardio.org/vpo/News/events/wcc\\_drugelutingstents\\_events.htm](http://www.escardio.org/vpo/News/events/wcc_drugelutingstents_events.htm)>.
- [27] Boston scientific confirms long-term clotting risk of drug-eluting stents. Retrieved September 11, 2006 from Angioplasty.org website. <<http://www.ptca.org/news/2006/0907.html>>.
- [28] Shirota T, Yasui H, Shimokawa H, Matsuda T. Fabrication of endothelial progenitor cell (EPC)-seeded intravascular stent devices and in vitro endothelialization on hybrid vascular tissue. *Biomaterials* 2003;24(13):2295–302.
- [29] Walter DH, Cejna M, Diaz-Sandoval L, Willis S, Kirkwood L, Stratford PW, et al. Local gene transfer of phVEGF-2 plasmid by gene-eluting stents. *Circulation* 2004;110(1):36–45.
- [30] Aoki J, Serruys PW, Van Beusekom H, Ong ATL, McFadden EP, Sianos G, et al. Endothelial progenitor cell capture by stents coated with antibody against CD34 – the HEALING-FIM (healthy endothelial accelerated lining inhibits neointimal growth – first in man) registry. *J Am Coll Cardiol* 2005;45(10):1574–9.
- [31] Tanquay JF. Vascular healing after stenting: the role of 17-beta-estradiol in improving re-endothelialization and reducing restenosis. *Can J Cardiol* 2005;21(12):1025–30.
- [32] Anis RR, Karch KR. The future of drug eluting stents. *Heart* 2005;92(5):585–8.
- [33] Cho HJ, Kim TY, Cho HJ, Park KW, Zhang SY, Kim JH, et al. The effect of stem cell mobilization by granulocyte-colony stimulating factor on neointimal hyperplasia and endothelial healing after vascular injury with bare-metal versus paclitaxel-eluting stents. *J Am Coll Cardiol* 2006;48(2):366–74.
- [34] Pelisek J, Fuchs AT, Kuehnl A, Tian W, Kuhlmann MT, Choukri M, et al. C-type natriuretic peptide for reduction of restenosis: gene transfer is superior over single peptide administration. *J Gene Med* 2006;8(7):835–44.
- [35] Patel HJ, Su S-H, Patterson C, Nguyen KT. A combined strategy to reduce restenosis for vascular tissue engineering applications. *Bio-technol Prog* 2006;22(1):38–44.
- [36] March KL, Trapnell BC. Pharmacokinetics of local viral vector delivery to vascular tissues: Implications for efficiency and localization of transduction. In: March K L, editor. *Gene transfer in the cardiovascular system: experimental approaches and therapeutic implications*. Dordrecht: Kluwer; 1997. p. 483.
- [37] March KL, Gradus-Pizlo I, Wilensky RL, Yei S, Trapnell BC. Cardiovascular gene therapy using adenoviral vectors: distant transduction following local delivery using a porous balloon catheter. *J Am Coll Cardiol* 1994;23(1):177A.
- [38] Choudhary S, Berhe M, Haberstroh KM, Webster TJ. Increased endothelial and vascular smooth muscle cell adhesion on nanostructured Ti and CoCrMo. *Int J Nanomed* 2006;1(1):41–9.
- [39] Parker ER, Thibeault BJ, Aimi MF, Rao MP, MacDonald NC. Inductively coupled plasma etching of bulk Ti for MEMS applications. *J Electrochem Soc* 2005;152(10):675–83.
- [40] Webster TJ, Ejirofor JU. Increased osteoblast adhesion on nanophase metals: Ti, Ti6Al4V, CoCrMo. *Biomaterials* 2004;25(19):4731–9.
- [41] Kathuria YP. Laser microprocessing of metallic stent for medical therapy. *J Mater Process Tech* 2005;170(3):545–50.
- [42] Takahata K, Gianchandani YB. A planar approach for manufacturing cardiac stents: design, fabrication, and mechanical evaluation. *J Microelectromech S* 2004;13(6):933–9.
- [43] Ingber DE, Madri JA, Folkman J. Endothelial growth factors and extracellular matrix regulate DNA synthesis through modulation of cell and nuclear expansion. *In Vitro Cell Dev Biol* 1987;23(5):387–94.
- [44] Palmaz JC, Benson A, Eugene A. Influence of surface topography on endothelialization of intravascular metallic material. *J Vasc Interv Radiol* 1999;10(4):439–44.
- [45] Ben-Ze'ev A. Animal cell shape changes and gene expression. *Bioassays* 1991;13(5):201–12.
- [46] Bettinger CJ, Orrick B, Misra A, Langer R, Borenstein JT. Micro fabrication of poly (glycerol-sebacate) for contact guidance applications. *Biomaterials* 2006;27(12):2558–65.
- [47] Khakbaznejad A, Chehroudi B, Brunette DM. Effects of titanium-coated micromachined grooved substrata on orienting layers of osteoblast-like cells and collagen fibers in culture. *J Biomed Mater Res* 2004;70(2):206–18.
- [48] Clark P, Connolly P, Curtis ASG, Dow JAT, Wilkinson CDW. Cell guidance by ultrafine topography in vitro. *J Cell Sci* 1991;99:73–7.